JACC Vol. 19, No. 1
January 1992:84–90

Doppler Echocardiographic Demonstration of the Differential Effects of Right Ventricular Pressure and Volume Overload on Left Ventricular Geometry and Filling

ERIC K. LOUIE, MD, FACC, STUART RICH, MD, FACC,* SIDNEY LEVITSKY, MD, FACC,†
BRUCE H. BRUNDAGE, MD, FACC‡

Maywood and Chicago, Illinois; Boston, Massachusetts; and Torrance, California

To compare the effects of isolated right ventricular pressure and volume overload on left ventricular diastolic geometry and filling, 11 patients with primary pulmonary hypertension, 11 patients with severe tricuspid regurgitation due to tricuspid valve resection and 11 normal subjects were studied with use of Doppler echocardiographic techniques. Right ventricular systolic overload in primary pulmonary hypertension resulted in substantial leftward ventricular septal shift that was most marked at end-systole and early diastole and decreased substantially by end-diastole. Right ventricular diastolic overload after tricuspid valve resection resulted in maximal leftward ventricular septal shift at end-diastole sparing end-systole and early diastole. The early diastolic distortion of left ventricular geometry associated with right ventricular pressure overload resulted in prolongation of isovolumetric relaxation of the left ventricle (129 ± 39 ms) and a reduction in early diastolic filling compared with values in normal subjects.

Late diastolic distortion of left ventricular geometry associated with right ventricular volume overload had no influence on the duration of left ventricular isovolumetric relaxation (82 ± 32 ms) but caused a reduction in the atrial systolic contribution to late diastolic filling of the left ventricle compared with values in normal subjects. In patients with right ventricular pressure overload, 52 ± 16% of left ventricular filling occurred in early diastole compared with 78 ± 11% in patients with right ventricular volume overload ($p < 0.001$). The differential effects of systolic and diastolic right ventricular overload on the pattern of left ventricular filling appear to be related to the timing of leftward ventricular septal displacement.

(J Am Coll Cardiol 1992;19:84–90)

Acute and chronic alterations in right ventricular loading influence left ventricular function because the two ventricles pump in *series* and because they are anatomically arranged in *parallel* sharing the common ventricular septum. Previous investigators (1–6) have demonstrated in right ventricular volume overload that the right ventricle fills at the expense of the left ventricle as the two chambers compete for space within extracardiac constraints to cardiac expansion. Under these conditions, the normally circular left ventricular short-axis profile becomes deformed because of end-diastolic leftward displacement of the ventricular septum into the left ventricle. These changes also occur in normal persons in whom right ventricular filling is augmented by the Mueller maneuver (7,8). Systolic overload of the right ventricle results in end-systolic leftward displacement of the ventricular septum as the left to right transventricular septal systolic pressure differential decreases or becomes reversed (3,9–12). Although reversal of ventricular septal curvature is most marked at end-systole, the deformation of left ventricular geometry persists throughout diastole with a variable degree of restoration toward normal by end-diastole. These changes are reversible, as demonstrated by echocardiographic studies of ventricular septal curvature after hemodynamic resolution of acute pulmonary embolism (13,14) or after thromboendarterectomy for pulmonary hypertension due to chronic thromboembolic pulmonary disease (15–17). Accordingly, we undertook this study to directly compare the effects of right ventricular pressure and volume overload on left ventricular filling and diastolic geometry.

Methods

Study group. All patients gave informed consent for the study protocol, which had the prior approval of the University of Illinois Institutional Review Board. Eleven patients (mean age 33 ± 10 years) with unexplained pulmonary hypertension underwent a comprehensive evaluation to exclude secondary causes of pulmonary hypertension (18) and had no evidence for primary myocardial, valvular or coro-

From the Section of Cardiology, Loyola University Medical Center, Maywood, Illinois; *Section of Cardiology, University of Illinois, Chicago, Illinois; †Division of Cardiothoracic Surgery, New England Deaconess Hospital, Harvard Medical School, Boston, Massachusetts; ‡Division of Cardiology, Harbor-UCLA Medical Center, Torrance, California. This report was presented in part at the 38th Scientific Session of the American College of Cardiology, Anaheim, California, March 22, 1989.

Manuscript received April 17, 1991; revised manuscript received June 18, 1991, accepted July 12, 1991.

Address for reprints: Eric K. Louie, MD, Section of Cardiology, Loyola University Medical Center, 2160 South First Avenue, Maywood, Illinois 60153.

0735-1097/92/$5.50

nary artery disease. Each patient underwent right heart catheterization simultaneously with the Doppler echocardiographic study. Mean pulmonary artery pressure was 53 ± 14 mm Hg, mean right atrial pressure was 5 ± 5 mm Hg and mean pulmonary capillary wedge pressure was 8 ± 2 mm Hg. Patients were selected for the presence of no greater than mild tricuspid regurgitation as assessed by pulsed Doppler mapping.

Eleven patients (mean age 33 ± 8 years) with severe tricuspid regurgitation resulting from tricuspid valvulectomy for isolated tricuspid valve infective endocarditis provided a group of patients with severe right ventricular volume overload to compare with the patients with right ventricular pressure overload due to primary pulmonary hypertension. None of these patients had evidence of cardiac disease before tricuspid valve endocarditis and subsequent tricuspid valvulectomy. All had a markedly elevated central venous pressure (estimated from the vertical height of the meniscus of the internal jugular venous pulsations, assuming that the sternal angle was 5 cm above the center of the right atrium) of 14 ± 4 mm Hg, which was significantly increased compared with that in the patients with primary pulmonary hypertension ($p < 0.001$). None of these patients with severe tricuspid regurgitation had evidence of pulmonary hypertension because in each patient the peak velocity of tricuspid regurgitation assessed by continuous wave Doppler echocardiography was ≤2.0 m/s (right ventricular to right atrial peak systolic pressure differential ≤16 mm Hg, hence right ventricular systolic pressure ≤30 ± 4 mm Hg).

Eleven normal subjects (mean age 32 ± 8 years) without myocardial or valvular disease by pulsed Doppler and two-dimensional echocardiography served as control subjects. A report (6) describing the patients with tricuspid valvulectomy and the normal subjects has been published previously).

Two-dimensional echocardiographic examination. Subjects were examined while they were in sinus rhythm, breathing quietly in the left lateral recumbent position. Two-dimensional echocardiograms from standard left parasternal and apical windows and pulsed Doppler ultrasound recordings were performed with use of a Diasonics CV 400 sector scanner (Diasonics) interfaced with a 3.5 MHz mechanical transducer. Parasternal short-axis two-dimensional echocardiographic images of the left ventricular cavity at the mitral leaflet, mitral chordal and papillary muscle levels were obtained by angling the transducer from base to apex. Orthogonality of these imaging planes to the left ventricular long axis was assessed by adjusting transducer angulation so that the medial and lateral aspects of the mitral commissures were symmetric at the mitral leaflet level. Stop frame images from the mitral chordal level of the left ventricle were selected for analysis as follows: 1) end-systole: stop frame demonstrating the smallest left ventricular cavity area just before the opening motion of the mitral chordal and leaflet tips; 2) end-diastole: stop frame demonstrating the maximal left ventricular cavity area just before the closing motion of the mitral chordal and leaflet tips; 3) mid-diastole: stop frame image of the left ventricle at the end of the first half of diastole (determined by counting forward from the end-systolic frame one half of the total number of frames encompassing diastole). The boundaries of the left ventricular endocardium were defined by the internal interface of the left ventricular endocardium with the blood pool. To assess left ventricular cavity shape, the short-axis left ventricular cross-sectional images proximal and distal to the mitral chordal level were examined to ascertain that the cavity profile at the chordal level was representative of left ventricular shape at all levels in each individual.

Standard apical two- and four-chamber images of the left ventricle and atrium were obtained with the sector apex aligned to the left ventricular inflow tract and angled so that maximal left ventricular and atrial cavity areas were obtained. Left atrial cavity area was measured from the two orthogonal apical images by tracing the internal interface between the left atrial wall and the blood pool (transecting pulmonary veins at their orifices and using the plane of the mitral anulus to define the boundary between the left ventricle and left atrium). The long axis of the left atrium in each view was defined as the distance from the mid-point of the mitral orifice to the superior margin of the left atrial cavity. These measurements were obtained at end-systole at the time of maximal left atrial cavity size.

Pulsed Doppler echocardiographic examination. Transmitral inflow was recorded by positioning the transducer at the apical window to obtain a standard four-chamber view of the heart with clear visualization of the ventricular apex, mitral valve and left atrium. The pulsed Doppler cursor was positioned parallel to the left ventricular long axis, running from the ventricular apex to the midpoint of the mitral orifice and the sample volume was positioned at the level of the mitral anulus. Left ventricular outflow was recorded from the same apical window by angling the transducer anteriorly to record a four-chamber view of the heart including the left ventricular outflow tract. The pulsed Doppler cursor was aligned parallel to the outflow tract along a line running from the left ventricular apex to the midpoint of the aortic orifice with the sample volume positioned just below the aortic valve. Optimal alignment of the Doppler beam was judged to have been attained when (6,9) 1) a relatively pure audio signal tone was appreciated, 2) a reproducible display of the flow velocity envelope with minimal (<0.5 kHz) spectral broadening could be recorded, and 3) maximal peak flow velocities were measured. No correction was attempted for the angle between the Doppler cursor and the apparent direction of blood flow, and in all instances that angle was estimated to be <20°. In no instance did the recorded Doppler frequency shifts exceed the Nyquist limit for the range gate utilized. The pulsed Doppler spectra were recorded with a simultaneous lead II electrocardiogram (ECG) by a strip chart recorder scrolling at 50 mm/s.

Measurements and calculations. Left ventricular geometry and ventricular septal displacement were quantified by

JACC Vol. 19, No. 1
January 1992:84–90

measuring the eccentricity index of the short-axis profile of the left ventricular cavity (at the mitral chordal level) at end-systole, mid-diastole and end-diastole (19). The ventricular septum was defined as that arc of the left ventricular circumference delimited by the attachments of the right ventricular free walls. A chord connecting the anterior and posterior boundaries of the ventricular septum along the left ventricular endocardial surface was constructed. The distance along the perpendicular bisector to that chord from the ventricular septal endocardium to left ventricular free wall endocardium defined the minor-axis diameter (D_1). The orthogonal minor-axis diameter (D_2) measuring the distance between anterior and posterior left ventricular endocardial surfaces, was measured and D_2/D_1 (= left ventricular cavity eccentricity index) was calculated. For an ideal circular left ventricular cavity, the eccentricity index would be 1 but with progressive flattening and leftward shift of the ventricular septum the eccentricity index would by >1.

Left atrial volume was derived from measurements of left atrial cavity area (A) and long-axis dimension (L) measured in two orthogonal planes sharing a common long-axis (apical two-chamber plane [2] and apical four-chamber plane [4]) with use of the area-length formula for a prolate ellipsoid (18,19):

$$\text{Volume} = 0.849 \frac{A_2 \times A_4}{L_{min}},$$

where L_{min} is the smaller of L_2 and L_4. Maximal left atrial volume normalized for body surface area was derived from left atrial stop frame images corresponding approximately to ventricular end-systole. All echocardiographic measurements were performed with a video screen digitizer interfaced to a computerized graphics analyzer (Nova MicroSonics Data Vue System, MicroSonics).

Doppler spectra of left ventricular outflow and mitral inflow were analyzed by digitizing the portion of the Doppler flow velocity spectrum with greatest intensity defining the instantaneous modal flow velocity profiles from which all subsequent measurements were derived. The time interval from the onset of the QRS complex of the ECG to the end of the systolic left ventricular flow velocity profile (QA) and the time interval from the onset of the QRS complex to the beginning of the diastolic transmitral flow velocity profile (QM) were measured from separate tracings with matched cycle lengths. The time interval from aortic valve closure to mitral valve opening (isovolumetric relaxation period) was calculated as QM−QA (6,9). The duration of the diastolic filling period was measured as the time interval from the beginning to the end of the transmitral flow velocity profile.

Peak mitral flow velocities in early diastole (V_E) and late diastole (V_A) were measured from the midpoint of the Doppler spectral envelope at the times of maximal Doppler shift during the *early* rapid filling phase and *atrial* systolic phase of left ventricular diastole. Stroke distance (SD) was measured by numeric integration of the area under the transmitral flow velocity profile. Assuming that the effective hemodynamic cross-sectional area at the mitral anulus (CSA) is constant throughout diastole, peak left ventricular filling rate in early diastole [PFR(E)] expressed in stroke volumes/s was computed as (20):

$$\text{PFR (E)} = \frac{V_E \times CSA}{SD \times CSA} = \frac{V_E}{SD}.$$

Similarly, peak filling rate in late diastole [PFR(A)] was computed as V_A/SD. To quantitate the relative contributions of the early (rapid) filling phase and the late (atrial systolic) filling phase of diastole to total left ventricular filling, the transmitral flow velocity integral for each of these two periods was determined by numeric integration (6,9). The fractional flow velocity integrals for the early and atrial filling phases of diastole were derived by dividing the respective flow velocity integrals for these two phases by stroke distance. All Doppler echocardiographic measurements were performed by digitizing hard copy with a Hitachi Tablet Digitizer (HDG-11B, Hitachi America) interfaced to an IBM AT microprocessor (International Business Machines) with use of a digitizing utility, VISHNU (Visual Numerics).

Statistical methods. The data were analyzed by one-way analysis of variance and, where appropriate, comparisons were tested with the Student's paired or unpaired *t* test. Two-tailed probability (p) values <0.05 were considered statistically significant. Data are reported as mean values ± 1 SD.

Results

Left Ventricular Diastolic Geometry

Normal subjects. For the 11 control subjects, the left ventricular cavity retained a nearly circular short-axis profile throughout the cardiac cycle. Consequently, the left ventricular eccentricity index varied minimally from unity (the value for a circle) at end-systole (1 ± 0.05), mid-diastole (1.03 ± 0.09) and end-diastole (1.03 ± 0.1) (p = NS for all comparisons).

Right ventricular pressure overload. For the 11 patients with primary pulmonary hypertension, left ventricular short-axis geometry was severely distorted by a marked leftward shift of the ventricular septum toward the center of the left ventricle. This resulted in flattening or reversal of the ventricular septal curvature (endocardial surface of the ventricular septum convex to the center of the left ventricular cavity) that was most pronounced in early diastole and returned toward normal in late diastole (Fig. 1). The average eccentricity index at end-systole was 1.64 ± 0.48, reflecting this marked distortion of left ventricular geometry just before the onset of left ventricular filling. This distortion decreased throughout the first half of diastole, resulting in a significant reduction of the left ventricular eccentricity index

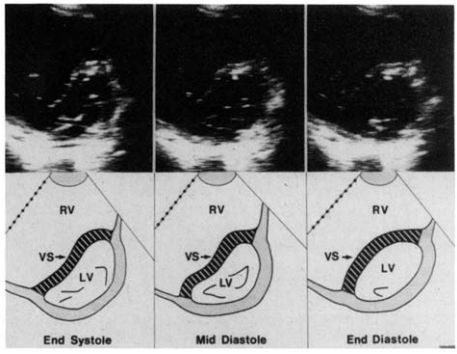

Figure 1. Stop frame two-dimensional echocardiographic images **(upper panel)** of the left ventricle in short-axis cross section at the level of the mitral chordae tendineae with diagrams below from a patient with primary pulmonary hypertension. Whereas the left ventricular (LV) cavity maintains a circular profile throughout the cardiac cycle in normal subjects, in this patient with right ventricular (RV) pressure overload there is leftward ventricular septal (VS) shift and reversal of septal curvature that is maximal at end-systole but persists well into mid-diastole. By end-diastole there is substantial, though incomplete, restoration of ventricular septal curvature.

to 1.32 ± 0.22 ($p < 0.03$ compared with the index at end-systole) by mid-diastole, but reflecting persistently abnormal leftward shift of the ventricular septum. At end-diastole, average left ventricular eccentricity index (1.33 ± 0.33) remained unchanged (by comparison with mid-diastole) for the group as a whole. However, in 4 of the 11 patients near normal eccentricity indexes ranging from 1.02 to 1.09 were attained by end-diastole.

Right ventricular volume overload. For the 11 patients with severe tricuspid regurgitation after tricuspid leaflet resection, the temporal sequence of geometric distortion was different (Fig. 2). The end-systolic left ventricular cavity short-axis profile was essentially circular in 8 of the 11 patients with eccentricity indexes ranging from 0.95 to 1.09. The remaining three patients exhibited mild degrees of leftward ventricular septal shift at end-systole, resulting in eccentricity indexes ranging from 1.16 to 1.21. The average end-systolic eccentricity index for all 11 patients with severe tricuspid regurgitation was 1.07 ± 0.09. During the course of diastole, progressive leftward shift of the ventricular septum was noted in each of the 11 patients resulting in flattening of the ventricular septum but not reversal of ventricular septal curvature. The left ventricular eccentricity index increased to 1.3 ± 0.23 ($p < 0.02$ compared with end-systole) at mid-diastole and to 1.25 ± 0.14 at end-diastole. All 11 patients with right ventricular volume overload had abnormal end-diastolic leftward ventricular septal displacement, whereas 4 of 11 patients with right ventricular pressure overload had relatively normal left ventricular septal configuration at end-diastole.

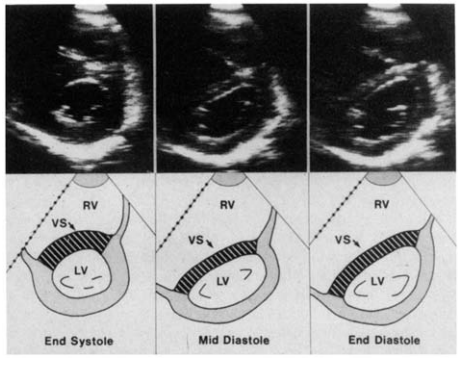

Figure 2. Stop frame two-dimensional echocardiographic images **(upper panel)** of the left ventricle in short-axis cross section at the level of the mitral chordae tendineae with diagrams below from a patient who had undergone tricuspid valvulectomy. In contrast to the patient with right ventricular pressure overload (Fig. 1), this patient with right ventricular (RV) volume overload due to severe tricuspid regurgitation exhibits maximal leftward ventricular septal (VS) shift between mid- and end-diastole. Although the *absolute* degree of septal distortion at end-diastole is similar in the patient with right ventricular volume overload and the patient with right ventricular pressure overload (Fig. 1), the *relative* severity of left ventricular (LV) distortion is most marked in *late diastole* for the patient with right ventricular *volume* overload and in *early diastole* for the patient with right ventricular *pressure* overload.

JACC Vol. 19, No. 1
January 1992:84–90

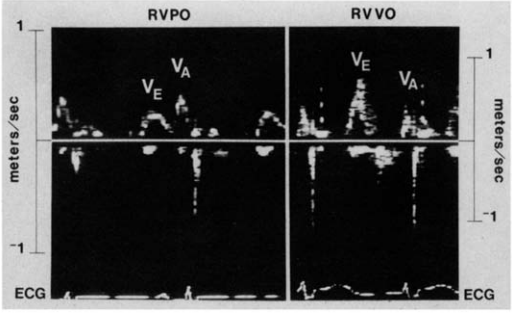

Figure 3. Pulsed Doppler transmitral flow velocity profiles from a patient with right ventricular pressure overload (RVPO) due to primary pulmonary hypertension **(left panel)** and a patient with right ventricular volume overload (RVVO) due to severe tricuspid regurgitation after tricuspid valvulectomy **(right panel)**. The patient with right ventricular pressure overload has an abnormal pattern of left ventricular filling with marked attenuation of the peak early filling velocity (V_E) and abnormal augmentation of the peak late filling velocity attributable to atrial systole (V_A). The reciprocal pattern of left ventricular filling is noted for the patient with right ventricular volume overload where peak early filling velocity (V_E) is accentuated and peak late filling velocity (V_A) is reduced. The areas under the portions of the flow velocity profiles attributed to early and late left ventricular filling are an index of the relative filling contributions from these two portions of diastole. Thus, in right ventricular pressure overload early diastolic left ventricular filling is impaired with redistribution of filling to late diastole and increased dependence on atrial systole. In right ventricular volume overload, late diastolic left ventricular filling due to atrial systole is reduced and early diastolic filling is relatively enhanced.

Left Atrial Volume

Maximal left atrial volume (at the end of ventricular systole) was not significantly different between the 11 patients with right ventricular pressure overload (14.5 ± 5.6 cc/m^2) and the 11 patients with right ventricular volume overload (14.6 ± 5.9 cc/m^2; p = NS). However, maximal left atrial volume in the 11 normal subjects was significantly greater than that measured in the two other patient groups, averaging 25.8 ± 7.3 cc/m^2 (p < 0.001 vs. each of the other patient groups).

Left Ventricular Filling Patterns

Normal subjects. For the 11 control subjects, mean cardiac cycle length was 856 ± 183 ms, diastolic filling period was 459 ± 174 ms and isovolumetric relaxation period was 70 ± 25 ms. Peak early diastolic mitral flow velocity (V_E) was 52 ± 10 cm/s, corresponding to a peak early filling rate (PFR_E) of 6.7 ± 2.0 stroke volumes/s. Peak late diastolic mitral flow velocity at the time of atrial systole (V_A) was 38 ± 8 cm/s, corresponding to a peak filling rate during atrial systole (PFR_A) of 4.9 ± 1.6 stroke volumes/s. The ratio of PFR_A/PFR_E was 0.72 ± 0.12.

Right ventricular pressure overload (Fig. 3). For the 11 patients with primary pulmonary hypertension, mean cardiac cycle length was 766 ± 100 ms and diastolic filling period was 334 ± 61 ms. The isovolumetric relaxation period was significantly prolonged compared with that of normal subjects (129 ± 39 vs. 70 ± 25 ms; p < 0.001). Mean V_E was 32 ± 14 cm/s, corresponding to a mean peak early filling rate (PFR_E) of 4.9 ± 0.8 stroke volumes/s. Mean V_A was 44 ± 12 cm/s corresponding to a mean peak filling rate during atrial systole (PFR_A) of 7.9 ± 4.4 stroke volumes/s. The ratio of PFR_A/PFR_E was significantly increased over the value for normal subjects (1.62 ± 0.93 vs. 0.72 ± 0.12; p < 0.005).

Right ventricular volume overload (Fig. 3). For the 11 patients with severe tricuspid regurgitation due to tricuspid leaflet resection, mean cardiac cycle length was 662 ± 150 ms and diastolic filling period was 293 ± 101 ms. The isovolumetric relaxation period (52 ± 32 ms) was not significantly different from the value for normal subjects, but significantly shorter than the isovolumetric relaxation period measured in patients with right ventricular pressure overload (p < 0.001). Mean V_E was 51 ± 18 cm/s corresponding to a mean PFR_E of 7.9 ± 2.3 stroke volumes/s. Mean V_A was 28 ± 11 cm/s corresponding to a mean PFR_A of 4.0 ± 1.1 stroke volumes/s. The ratio of PFR_A/PFR_E (0.54 ± 0.20) was significantly decreased with respect to values for patients with right ventricular pressure overload (p < 0.002) and normal subjects (p < 0.02).

Comparison of fractional flow velocity integrals in the three groups. The relative contributions to left ventricular filling of early diastole and late diastole (predominantly reflecting the contribution of atrial systole) were assessed by comparing the early and atrial fractional flow velocity integrals in these three groups of subjects. Normal subjects had a mean early fractional flow velocity integral of 0.68 ± 0.09 and a mean atrial fractional flow velocity integral of 0.32 ± 0.09. In contrast, patients with right ventricular pressure overload had a relative shift of left ventricular filling to late diastole

when compared with findings in normal subjects. Accordingly, the mean early fractional flow velocity integral was significantly decreased (0.52 ± 0.16, $p < 0.01$) and the mean atrial fractional flow velocity integral was proportionately increased (0.48 ± 0.16, $p < 0.01$) relative to values in normal subjects. The reverse pattern was seen in patients with right ventricular volume overload, who had a relative shift of left ventricular filling to early diastole compared with findings in normal subjects. Accordingly, the mean early fractional flow velocity integral was increased (0.78 ± 0.11, $p < 0.04$) and the mean atrial fractional flow velocity integral was proportionately decreased (0.22 ± 0.11, $p < 0.04$) relative to values in normal subjects. Thus, a significantly greater proportion of left ventricular filling occurred in early diastole in patients with right ventricular diastolic overload compared with patients with right ventricular systolic overload (0.78 ± 0.11 vs. 0.52 ± 0.16, $p < 0.001$).

Discussion

Ventricular interdependence in right ventricular pressure and volume overload. During cardiopulmonary bypass the unloaded human heart free of external constraints to filling (open chest and pericardium) assumes a partially collapsed underfilled state (21). Under these conditions, short-axis cross-sectional profiles of the left ventricle reveal that the ventricular septum is relatively flat, taking on a neutral position between the two ventricles dictated by the unstressed configuration of the cardiac muscle fibers that constitute the ventricular septum and the contiguous ventricular chambers. Under physiologic conditions systolic and diastolic loading of the left ventricle exceeds that of the right ventricle and the ventricular septum becomes concave with respect to the center of the left ventricular cavity, resulting in a relatively circular short-axis cross-sectional left ventricular profile (21,22). As demonstrated in the current study, isolated right ventricular volume overload results in diastolic loading of the right ventricle, with the most marked geometric distortion of the ventricular septum at end-diastole when the right ventricle is maximally distended. This late diastolic deformation of left ventricular geometry results in a reduction in late diastolic left ventricular filling during atrial systole compared with findings in normal subjects. In contrast, systolic overload of the right ventricle resulted in the most severe geometric distortion of the left ventricle at end-systole. This resulted in maximal leftward displacement of the ventricular septum, flattening or reversal of ventricular septal curvature and compression of the left ventricle at end-systole. Leftward ventricular septal shift present at end-systole persisted into early diastole, with restoration of more normal left ventricular geometry by end-diastole.

Thus, whereas *diastolic* overload of the right ventricle resulted in disproportionate *late* diastolic distortion of the left ventricle, *systolic* overload of the right ventricle resulted in disproportionate *early* diastolic distortion of left ventricular geometry. The early diastolic leftward ventricular septal shift induced by systolic loading of the right ventricle was associated with prolongation of left ventricular isovolumetric relaxation and a redistribution of left ventricular filling from early to late diastole, whereas the late diastolic leftward ventricular septal shift induced by diastolic loading of the right ventricle redistributed left ventricular filling from late to early diastole without influencing the left ventricular isovolumetric relaxation period.

Alternative mechanisms to explain the impact of right ventricular loading on left ventricular filling. Although these observations suggest that the timing of interaction through the ventricular septum influences the impact of right ventricular loading on left ventricular filling, there remains the possibility that differences in left ventricular preload might explain the differing patterns of left ventricular filling found in this study. Reduction in right ventricular output in either primary pulmonary hypertension (9,18) or severe tricuspid regurgitation (16) could result in decreased left ventricular preload (as reflected in the significant reduction in left atrial volume of the two patient groups relative to values in normal subjects). Also, interatrial interaction through the atrial septum in patients with severe tricuspid regurgitation serves to reduce left atrial filling (6). However, it seems unlikely that impaired left atrial filling and reduced left ventricular preload *alone* can explain the differences in left ventricular filling patterns seen in this study because maximal left atrial volume, an index of left atrial filling, did not differ significantly between the patients with primary pulmonary hypertension and those who had undergone tricuspid valve resection.

Systolic and diastolic loading of the right ventricle could result in different intrinsic morphologic responses in the myocardium of the shared ventricular septum that could partially account for the observed differences in left ventricular filling. However, the *acute* normalization of left ventricular filling patterns after relief of right ventricular pressure overload by pulmonary thromboendarterectomy (16,17) suggests that restoration of left ventricular geometry, and not regression of right ventricular hypertrophy, is responsible for the normalization of early left ventricular filling. Similarly, tricuspid valvulectomy results in *acute* induction of tricuspid regurgitation and right ventricular volume overload. Our previous observations in patients who have undergone tricuspid valvulectomy suggest that acute distortion of left ventricular geometry, and not intrinsic myocardial responses to diastolic loading, accounts for the reduction in late diastolic left ventricular filling compared with values in normal subjects (6).

Methodologic considerations. Analysis of ventricular septal motion can be separated into two components: displacement of the septum due to anterior systolic translation of the entire heart and intrinsic septal geometric changes relative to a floating frame of reference, the center of the left ventricular cavity. Although translational motion of the heart is minimal in patients with right ventricular pressure overload, it is a significant component of ventricular septal motion relative to

JACC Vol. 19, No. 1
January 1992:84–90

an external frame of reference in patients with right ventricular volume overload (3). Similarly, the "abnormal septal motion" after cardiac surgery measured relative to a fixed external frame of reference is due to translation and rotation of the untethered cardiac structures rather than to intrinsic distortion of septal geometry and can be eliminated by employing an internal floating frame of reference (23). Accordingly, in this study we measured the left ventricular eccentricity index, which employs an internal floating frame of reference (19) and thus eliminates the extraneous effects of cardiac translation and rotation seen in right ventricular volume overload (1,3) and in the postcardiac surgery state (23), permitting analysis of the intrinsic effect of right ventricular loading on septal geometry.

Conclusions. Right ventricular systolic overload distorts early diastolic left ventricular geometry, delays left ventricular isovolumetric relaxation and impedes the rapid filling phase of left ventricular filling. In contrast, right ventricular diastolic overload results in late diastolic distortion of the left ventricle as the two chambers compete for filling within extracardiac and intrathoracic constraints, resulting in reduced late diastolic left ventricular filling. Diastolic ventricular interdependence by means of geometric interaction through the common ventricular septum appears to be the primary determinant of these alterations in patterns of left ventricular filling.

References

1. Weyman AE, Wann S, Feigenbaum H, Dillon JC. Mechanisms of abnormal septal motion in patients with right ventricular volume overload. Circulation 1976;54:179–86.
2. Shimada R, Takeshita A, Nakamura M. Noninvasive assessment of right ventricular systolic pressure in atrial septal defect: analysis of the end-systolic configuration of the ventricular septum by two-dimensional echocardiography. Am J Cardiol 1984;53:1117–23.
3. Feneley M, Gavaghan T. Paradoxical and pseudoparadoxical interventricular septal motion in patients with right ventricular volume overload. Circulation 1986;74:238–8.
4. Benson LN, Child JS, Schwaiger M, Perloff JK, Schelbert HR. Left ventricular geometry and function in adults with Ebstein's anomaly of the tricuspid valve. Circulation 1987;75:353–9.
5. Lasseur SI, Tani L, Jawad I. Pattern of left ventricular filling associated with right ventricular enlargement. Am J Cardiol 1988;62:444–8.
6. Louie EK, Bleniarz T, Moore AM, Lewitsky S. Reduced atrial contribution to left ventricular filling in patients with severe tricuspid regurgitation after tricuspid valvulectomy: a Doppler echocardiographic study. J Am Coll Cardiol 1990;16:1617–24.
7. Brinker JA, Weiss JL, Lapoe DL, et al. Leftward septal displacement during right ventricular loading in man. Circulation 1980;61:626–33.
8. Guzman PA, Monaghan WL, Yin FCP, et al. Transseptal pressure gradient with leftward septal displacement during the Mueller manoeuvre in man. Br Heart J 1981;46:657–62.
9. Louie EK, Rich S, Brundage BH. Doppler echocardiographic assessment of impaired left ventricular filling in patients with right ventricular pressure overload due to primary pulmonary hypertension. J Am Coll Cardiol 1986;8:1298–306.
10. Kasper W, Meinertz T, Henkel B, et al. Echocardiographic findings in patients with proved pulmonary embolism. Am Heart J 1986;112:1284–90.
11. Jessup M, St John Sutton MS, Weber KT, Janicki JS. The effect of chronic pulmonary hypertension on left ventricular size, function, and interventricular septal motion. Am Heart J 1987;113:1114–22.
12. Shuller BF, Colan SD, Sanders SP. Effect of isolated right ventricular outflow obstruction on left ventricular function in infants. Am J Cardiol 1988;62:778–84.
13. Come PC, Kim D, Parker JA, et al. Early reversal of right ventricular dysfunction in patients with acute pulmonary embolism after treatment with intravenous tissue plasminogen activator. J Am Coll Cardiol 1987; 10:971–8.
14. Jardin F, Dubourg O, Guéret P, Delorme G, Bourdarias J-P. Quantitative two-dimensional echocardiography in massive pulmonary embolism: emphasis on ventricular interdependence and leftward septal displacement. J Am Coll Cardiol 1987;10:1201–6.
15. Dittrich HC, Nicod PH, Chow LC, Chappuis FP, Moser KM, Peterson KL. Early changes of right heart geometry after pulmonary thromboendarterectomy. J Am Coll Cardiol 1988;11:937–43.
16. Dittrich HC, Chow LC, Nicod PH. Early improvement in left ventricular diastolic function after relief of chronic right ventricular pressure overload. Circulation 1989;80:823–830.
17. Dittrich HC, Nicod PH, Thomas TC, Dembitsky WP, Moser KM. Acute intraoperative changes in cardiac geometry and left ventricular diastolic filling during surgical reduction of severe right ventricular pressure overload in man (abstr). J Am Coll Cardiol 1990;15:244A.
18. Rich S, Dantzker DR, Ayres SM, et al. Primary pulmonary hypertension: a national prospective study. Ann Intern Med 1987;107:216–23.
19. Ryan T, Petrovic O, Dillon JC, Feigenbaum H, Conley MJ, Armstrong WF. An echocardiographic index for separation of right ventricular volume and pressure overload. J Am Coll Cardiol 1985;5:918–24.
20. Bowman LK, Lee FA, Jaffe CC, Mattera J, Wackers FJTH, Zaret BL. Peak filling rate normalized to mitral stroke volume: a new Doppler echocardiographic filling index validated by radionuclide angiographic techniques. J Am Coll Cardiol 1988;12:937–43.
21. Lima JAC, Guzman PA, Yin FCP, et al. Septal geometry in the unloaded living human heart. Circulation 1986;74:463–8.
22. Kaul S. The interventricular septum in health and disease. Am Heart J 1986;112:568–81.
23. Force T, Bloomfield P, O'Boyle JE, et al. Quantitative two-dimensional echocardiographic analysis of motion and thickening of the interventricular septum after cardiac surgery. Circulation 1983;68:1013–20.